Theoretical Study of the Electronic Structure of $[TCNQ]_2^{2-}$ (TCNQ = 7,7,8,8-Tetracyano-*p*-quinodimethane) Dimers and Their Intradimer, Long, Multicenter Bond in Solution and the Solid State

Iñigo Garcia-Yoldi,[†] Joel S. Miller,*[,‡] and Juan J. Novoa*[,†]

Departament de Química Física and IQTCUB, Facultat de Química, Universitat de Barcelona, Av. Diagonal 647, 08028 Barcelona, Spain, and Department of Chemistry, University of Utah, Salt Lake City, Utah 84112-0850

Received: March 2, 2009; Revised Manuscript Received: May 4, 2009

The long, multicenter bonding in 7,7,8,8-tetracyano-*p*-quinodimethane anion radical dimers, $[TCNQ]_2^{2-}$, observed in both the solid state and in solution, was computationally investigated via B3LYP, CASSCF(2,2), and MCQDPT/CASSCF(2,2) methods. Isolated $[TCNQ]^{\bullet-}\cdots[TCNQ]^{\bullet-}$ interactions are repulsive by all three methods, although a metastable minimum is found at the MCQDPT/CASSCF(2,2) level. In the solid state, the stability of $[TCNQ]_2^{2-}$ dimers primarily originates from $[TCNQ]^{\bullet-}\cdots cation^+$ electrostatic interactions, whose sum exceeds the sum of the $[TCNQ]^{\bullet-}\cdots[TCNQ]^{\bullet-}$ and $cation^+\cdots anion^+$ repulsive interactions. In the solid state, as observed for $K_2[TCNQ]_2$ aggregates, $[TCNQ]_2^{2-}$ has a long, two-electron bond with contributions from 20 centers (4 N···N and 6 C···C). In solution, their stability originates from the $[TCNQ]^{\bullet-}$solvent attractive interactions, as calculated for $\{[TCNQ]_2(S)_4\}^{2-}$ (S = CH_2Cl_2, H_2O), and these have contributions from 16 C centers as the N atoms do not contribute because the nitriles bend away from the nominal plane of the fragment. MCQDPT/CASSCF(2,2) calculations indicate that the electronic ground state of these $[TCNQ]_2^{2-}$ dimers is a closed-shell singlet with a non-negligible contribution from the open-shell singlet, as is experimentally observed. This ground-state electronic structure is well described from B3LYP calculations.

Introduction

Tetracyanoethylene (TCNE) and 7,7,8,8-tetracyano-*p*-quinodimethane (TCNQ) are two of the most widely used electron acceptors in molecule-based electron transfer salts that frequently exhibit properties of technological interest, among them bulk magnetic ordering.[1] In some of these crystals, diamagnetic dianionic dimers, $[A]_2^{2-}$ (A = TCNE, TCNQ), have been reported. Whereas many examples of electron transfer salts possessing $[TCNE]^{\bullet-}$ exhibit bulk magnetic ordering,[2] and many examples of electron transfer salts possessing $[TCNQ]^{\bullet-}$ exhibit high metal-like dc electrical conductivity,[3] these properties are not manifested when $[A]_2^{2-}$ is present. Therefore, to obtain new $[TCNE]^{\bullet-}$ and $[TCNQ]^{\bullet-}$ electron transfer salts with technologically interesting properties, it is necessary to understand the factors that control the existence of $[TCNE]_2^{2-}$ and $[TCNQ]_2^{2-}$ dimers.

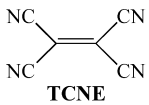

TCNE

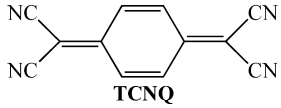

TCNQ

Interest in the $[A]_2^{2-}$ anion radical dimers also arises from their long, multicenter intradimer bonding, as first reported for $[TCNE]_2^{2-}$ dimers.[4–9] $[TCNE]_2^{2-}$ dimers exhibit all of the electronic properties of a conventional covalent bond, except for its intrinsic energetic stability. They are energetically stable because the sum of the attractive $cation^+\cdots anion^-$ interactions exceeds the sum of the repulsive $anion^-\cdots anion^-$ and $cation^+\cdots cation^+$ interactions. A smaller extra stabilization arises from the dispersion component present between the two ion radicals, as was first shown for $[TCNE]_2^{2-}$ dimers.[5,10] Long, multicenter bonds were later studied in other anion radical dimers (e.g., cyanil[11]), cation radical dimers (e.g., $[TTF]_2^{2+}$, TTF: tetrathiafulvalene[12]), and neutral radical dimers (e.g., phenalenyl[13]). The covalent-like properties of these long bonds originate from the overlap of the SOMO orbital of the radicals. The short intradimer separation allows the SOMOs on each fragment to overlap. For example, in $[TCNE]_2^{2-}$, the shortest interfragment C···C distance is 2.9 Å (~3.4 Å in $[TTF]_2^{2+}$,[12] which is similar to the shortest interfragment S···S distance). This overlap results in the formation of bonding and antibonding orbitals of these SOMOs that are, respectively, doubly occupied and empty in the singlet ground state. Therefore, these dimers have the same orbital diagram as that for conventional covalent bonds.[4]

Herein we extend our previous studies on $[A]_2^{2-}$ anion radical dimers to the $[TCNQ]_2^{2-}$ dimers and establish the origin of their stability in solids and in solution. The formation of cofacial $[TCNQ]_2^{2-}$ dimers has been experimentally reported[14–17] in solids and in solution.[14,16] In the solid state, these dimers have been reported to exhibit several structures,[14,17] with their shortest interfragment distance being ~3.3 Å, which is slightly less than the sum of the van der Waals radii for aromatic carbon.[18]

The geometry of all of these dimers was also statistically analyzed[17] by a search of the Cambridge Structure Database (CSD)[19] for all $[TCNQ]_2^n$ dimers, irrespective of their net charge (*n*), and also when one or more H atoms of the TCNQ fragments

* Corresponding authors. E-mail: jsmiller@chem.utah.edu (J.S.M.); juan.novoa@ub.edu (J.J.N.).
[†] Universitat de Barcelona.
[‡] University of Utah.

10.1021/jp901930s CCC: $40.75
Published on Web 06/02/2009

are substituted by atoms of another element. It was concluded that two types of π dimers existed, namely, π_L (**1**) and π_T (**2**), depending on the lateral or transverse displacement of one fragment with respect to the other. Furthermore, σ dimers with the shortest interfragment C−C distance of ∼1.6 Å were also reported,[20] as also occurs for reduced TCNE.[21] Therefore, reduced TCNQ can form both σ- and π-$[TCNQ]_2^{2-}$ dimers. Herein the latter π-$[TCNQ]_2^{2-}$ dimer is focused on; hence, $[TCNQ]_2^{2-}$ refers to π-$[TCNQ]_2^{2-}$. DFT calculations using a local density functional to study the energetic stability of the different $[TCNE]^{\bullet-}\cdots[TCNE]^{\bullet-}$ relative orientations that they found in the crystal as well as the stability of these dimers against their dissociation were performed.[17] (The $[TCNQ]_2^{2-}$ dimers were found to be metastable in their calculations.)

Although this CSD search identified structures that possessed the geometry of $[TCNQ]_2^{2-}$, they are mixed with more complex $[TCNQ]_3^{2-}$ structures[22] and with structures where the $[TCNQ]^{\bullet-}$ forms nondimeric regular stacks.[22] Therefore, a statistical analysis of only $[TCNQ]_2^{2-}$ dimers was made. It is also worth mentioning the review by Herbstein and Kapon where they analyzed the different crystal structures with TCNQ in their different oxidation states.[23]

The formation of $[TCNQ]_2^{2-}$ dimers was also reported to occur in water[14] and in dichloromethane[16] at room temperature. Spectroscopic (UV/vis and EPR) studies in these solvents have established the thermodynamic parameters for the $2[TCNQ]^{\bullet-} \leftrightarrows [TCNQ]_2^{2-}$ dimerization ($\Delta H_{dim} = -10.4$ kcal/mol and $\Delta S_{dim} = -19.5$ eu in water[14] and $\Delta H_{dim} = -9.8$ kcal/mol and $\Delta S_{dim} = -42$ eu in dichloromethane[16]). The dimerization was reversible but was solvent- and temperature-dependent. The absorption spectrum is similar to the reported spectrum of solid,[15e,16] being essentially invariant when the solvent or counterions were changed. This suggests that the structure of the $[TCNQ]_2^{2-}$ dimers is similar in solution and the crystal and also largely unaffected by the environment, as occurs for $[TCNE]_2^{2-}$.[24−26] The $[TCNQ]_2^{2-}$ dimers were also found to be diamagnetic.[15e,16,27]

To improve our knowledge of the origin of the stability of $[TCNQ]_2^{2-}$ in the solid state and in solution as well as of the nature of the long, intradimer bonding, we have studied the electronic structure of $[TCNQ]_2^{2-}$ for an isolated dimer and for dimers present in $K_2[TCNQ]_2$[28] and in water and dichloromethane solutions by combining B3LYP density functional, CASSCF(2,2), and MCQDPT/CASSCF(2,2) calculations. Therefore, we extend a previous study on the interaction energy of isolated $[TCNQ]_2^{2-}$ dimers that was done using a local density functional.[17]

Methodological Details. The characterization of the electronic structure and properties of $[TCNQ]_2^{2-}$ dimers was done in three consecutive steps. First, the interaction energy, $E(d)$, curve of an isolated $[TCNQ]_2^{2-}$ dimer as a function of the shortest interfragment C−C distance, d, was evaluated at the B3LYP density functional,[29] CASSCF(2,2),[30] and MCQDPT/CASSCF(2,2)[31,32] computational levels. The MCQDPT/CASSCF(2,2) method provides an accurate evaluation of the dispersion component of the interaction energy and gives results similar to those obtained using the more popular CASPT2 method.[33] Second, the energetic interactions in a representative crystal possessing $[TCNQ]_2^{2-}$ dimers were evaluated to identify the reasons behind the existence of the dimers in the solid state. The energetic evaluation was done on the $[cation]_2[TCNQ]_2$ aggregate, the smallest aggregate where all of the interactions are found in the $[K]_2[TCNQ]_2$ crystal.[28] Finally, we investigated the presence of $[TCNQ]_2^{2-}$ dimers in water and dichloromethane solutions by evaluating the intermolecular interactions in $\{[TCNQ]_2[H_2O]_n\}^{2-}$ and $\{[TCNQ]_2[CH_2Cl_2]_n\}^{2-}$ aggregates. The electronic structure of $[TCNQ]_2^{2-}$ in these calculations is rationalized in terms of the qualitative orbital diagrams that result from the overlap of the SOMO of two $[TCNQ]^{\bullet-}$ monomers (whose shape was obtained from UB3LYP/6-31+G(d) computations).

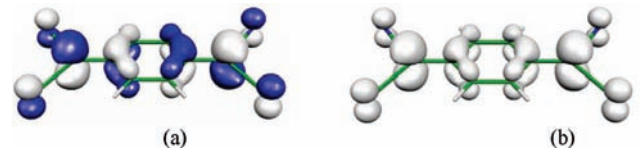

Figure 1. (a) Shape of the $[TCNQ]^{\bullet-}$ SOMO (blue and white regions represent areas where the orbital is positive and negative, respectively) obtained from a UB3LYP/6-31+G(d) calculation. (b) Shape of the spin density (the isosurface of ±0.05 atomic units; note the absence of regions of negative spin density). C, green; N, blue; H, white.

The CASSCF(2,2) and MCQDPT/CASSCF(2,2) methods were used because previous B3LYP computations on $[TCNE]_2^{2-}$ dimers failed to reproduce their diamagnetic ground state,[15b,16] a property that was well reproduced by MCQDPT/CASSCF(2,2) calculations. In these CASSCF(2,2) and MCQDPT/CASSCF(2,2) calculations, the (2,2) active space included the two SOMO orbitals of the fragments at dissociation. In this form, the closed-shell singlet, CSS, and open-shell singlet, OSS, states that can originate from the interaction of the two doublet radical cations can be can properly described.

All B3LYP calculations were done using the 6-31+G(d) basis set[34] and the Gaussian 03 suite of programs,[35] whereas the CASSCF(2,2) and MCQDPT/CASSCF(2,2) calculations were done using the GAMESS-07 suite of programs.[36] In all cases, the interaction energies were corrected by the basis set superposition error (BSSE) using the counterpoise method.[37]

Results and Discussion

To understand the electron structure of $[TCNQ]_2^{2-}$ dimers, we computed the electronic structure of the $[TCNQ]^{\bullet-}$ monomer at the UB3LYP/6-31+G(d) level, which is illustrated in Figure 1a. $[TCNQ]^{\bullet-}$ has a doublet ground state with its SOMO mostly located on the C atoms participating in C=C bonds and on the N atoms of the CN groups (Figure 1). The SOMO is in accord with that previously reported.[15a,38] The atomic spin population (Table S1 in the Supporting Information) indicates that most of the spin density is located on the $C(sp^2)$ atoms (0.31 e^-/$C(sp^2)$ atom), followed by 0.11 e^-/N atom, −0.07 e^-/C(sp) atom of the cyano groups, and 0.06 e^- per each substituted $C(sp^2)$ atoms of the six-membered ring. All other atoms have atomic spin populations smaller than |0.04 e^-|.

Nature of the $[TCNQ]^{\bullet-}\cdots[TCNQ]^{\bullet-}$ Interactions in Isolated $[TCNQ]_2^{2-}$ Dimers. The potential energy curves for an isolated $[TCNQ]_2^{2-}$ computed at the RB3LYP/6-31+G(d) and UB3LYP/6−3+G(d) levels are shown in Figure 2. We obtained the curves by optimizing the geometry of the dimer at each distance, d (the shortest central C−C distance). Both curves are energetically unstable with respect to the dissociation of the dimer into its fragments. A very small metastable minimum is found in the RB3LYP curve at ∼3.75 Å, although it disappears for the UB3LYP-computed curve. This suggests that it is due to the double occupancy restriction implicit in the RB3LYP calculations. The same trend was reported for the RB3LYP and UB3LYP curves computed for the $[TCNE]_2^{2-}$ and the $[TTF]_2^{2+}$ dimers.[4,5,10,12] The MCQDPT/CASSCF(2,2) curve is expected to give the highest quality results because this method is capable of describing the closed-shell/open-shell

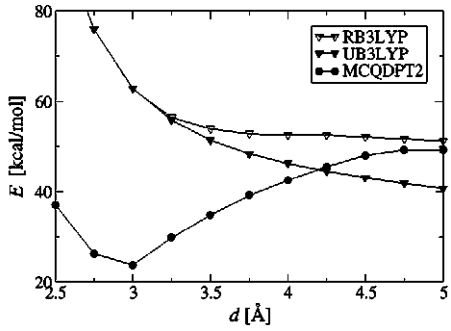

(a)

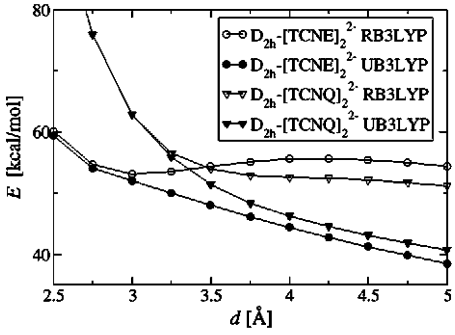

(b)

Figure 2. Computed variation of the interaction energy, $E(d)$, of two $[TCNQ]^{\bullet-}$ fragments placed in a D_{2h} geometrical arrangement as a function of interfragment C−C distance (d). (a) The curves are those for the lowest-energy singlet state computed at the RB3LYP, UB3LYP, and MCQDPT/CASSCF(2,2) computational levels. (b) Comparison with the curves computed at the RB3LYP, UB3LYP levels for the interaction energy of two $[TCNQ]^{\bullet-}$ fragments.

nature of the singlet ground state and makes a proper account of the dispersion component of the interaction energy.[30−33] This curve is also energetically unstable with respect to the dissociation of the dimer into its fragments and also has a metastable minimum at ∼3.2 Å, which is not found from the CASSCF(2,2) calculations (curve not shown in Figure 2). This indicates that the dispersion component of the interaction energy is qualitatively relevant. Therefore, the formation of isolated $[TCNQ]_2^{2-}$ dimers is not a spontaneous process. Hence, the presence of $[TCNQ]_2^{2-}$ dimers in the solid state and in solution is due to an environment where they can get enough energy to compensate for the intrinsic repulsive nature. In another words, the bonding component (E_{bond}) of the $[TCNQ]^{\bullet-}\cdots[TCNQ]^{\bullet-}$ interaction energy, which originates from the overlap of the two SOMO orbitals of the fragments, is less than the Coulombic $anion^-\cdots anion^-$ component (E_{el}) originating from their net negative charges. (Both are well described at the RB3LYP and UB3LYP levels.) The inclusion of the dispersion component for the optimum UB3LYP points, as done in the MCQDPT/CASSCF(2,2) curve, leads to a physically meaningful metastable minimum, although its formation still requires energy. Note that the metastable minimum was also reproduced by the local density studies of ref 17 with a similar geometry and stability as that of the MCQDPT/CASSCF(2,2)-computed curve.

Nature of the $[TCNQ]^{\bullet-}\cdots[TCNQ]^{\bullet-}$ Interactions in Crystals. The presence of $[TCNE]_2^{2-}$ and $[TTF]_2^{2+}$ dimers[4,12] is attributed to the existence of energetically stable aggregates that contain these dimers and whose stability originates in the $cation^+\cdots anion^+$ attractive interactions that exceed the sum of the $cation^+\cdots cation^+$ and $anion^-\cdots anion^-$ repulsive interactions (Figure 3).

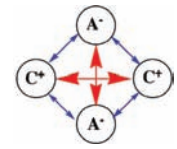

Figure 3. Schematic representation of the most important, first-neighbor pair interactions in $(cation)_2[TCNQ]_2$ aggregates. Cations are indicated as C^+ and anions are indicated as A^-.

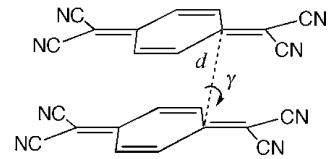

Figure 4. Definition of the intradimer separation, d, and dihedral angle, γ, employed to define the geometry of the $[TCNQ]^{\bullet-}\cdots[TCNQ]^{\bullet-}$ pairs. A π dimer occurs when $\gamma = 0°$, and a σ dimer occurs when $\gamma = 180°$ and $d < 1.9$ Å.

We identified suitable $(cation)_2[TCNQ]_2$ aggregates possessing short-distance $[TCNQ]_2^{2-}$ dimers by searching the CSD.[19] This search focused on identifying $[TCNQ]^{\bullet-}\cdots[TCNQ]^{\bullet-}$ pairs by looking for 2.0 to 4.0 Å C···C distances indicated in broken lines in Figure 4. By manual inspection, all pairs presenting neutral TCNQ molecules were discarded, as were all structures where $[TCNQ]^{\bullet-}$ radicals formed regular stacks. Sixty-eight crystal structures were identified as having dimers with the desired geometrical features. (Table S2 in the Supporting Information collects their CSD REFCODE, chemical formula, and values of the parameters d and γ and also gives their references.)

These structures can be grouped into three classes according to the values of the shortest interfragment C···C distance (d, Figure 4) involving the six-membered ring C atoms connected to the $C(CN)_2$ moiety and the dihedral angle (γ) (Figure 4), which correspond to σ dimers ($d \approx 1.6$ Å, $\gamma \approx 180°$), π_T ($d \approx 3.3$ Å, $\gamma \approx 0°$), and π_L ($d \approx 3.3$ Å, $\gamma \approx 180°$). These groups are similar to that reported for the TCNE analogs[4b] and were also located in an analysis by Kertesz and coworkers.[17] The largest group is π_T. Figure S1 in the Supporting Information shows the variation in d for all crystals of the π_T crystals subset as well as the correlation of d with the C−N distance in the CN group and with the out-of-plane CN dihedral angle. (Measured as C(13)−C11−C(1)−C(4) in Table S1 in the Supporting Information.) The maximum probability of d is ∼3.2 Å, whereas the C−N distances have in all but one case values close to 1.15 Å. Finally, it is worth pointing out the tendency toward the coplanarity of the CN groups with very small out-of-plane deviations (smaller than 7° usually). Note that besides the σ, π_T, and π_L groups, there is one dimer that has structure located between the π_T and π_L groups ($d = 3.46$ Å; $\gamma = 32.41°$), found in $[C_{18}H_{24}Cr^I]_2[TCNQ]_2$.[39]

Among the short-distance $[TCNQ]_2^{2-}$ dimers, $K_2[TCNQ]_2$[28] was selected for an in-depth study of its electronic structure properties (Figure 5). This dimer belongs to the π_T group ($d = 3.342$ Å, $\gamma = 0°$), and the shortest distance between pairs is 3.750 Å. The interaction energy of the aggregate against its dissociation into its four constituent fragments was computed at the RB3LYP level (thus, forcing the singlet to be a closed-shell singlet, CSS). A UB3LYP natural population analysis indicated an occupation of 1.7 and 0.3 electrons for the HOMO and LUMO orbitals. Therefore, the singlet ground state is mostly a CSS state with non-negligible contribution of the open-shell singlet (OSS). In other words, the B3LYP predicts a small OSS character in good agreement with the experimental data. Note

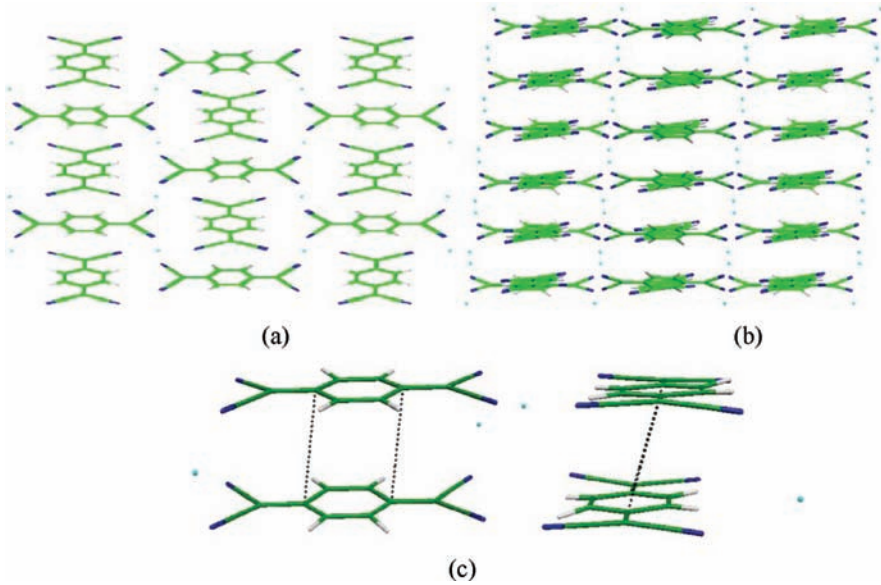

Figure 5. Structure of the $K_2[TCNQ]_2$ crystal (C, green; N, blue; H, white; K, cyan) (a) along the *a* axis and (b) along the *b* axis. (c) Two views of the geometry of the $K_2[TCNQ]_2$ aggregate used in the computations. (The dotted lines indicate the shortest interfragment C−C distance (3.342 Å).)

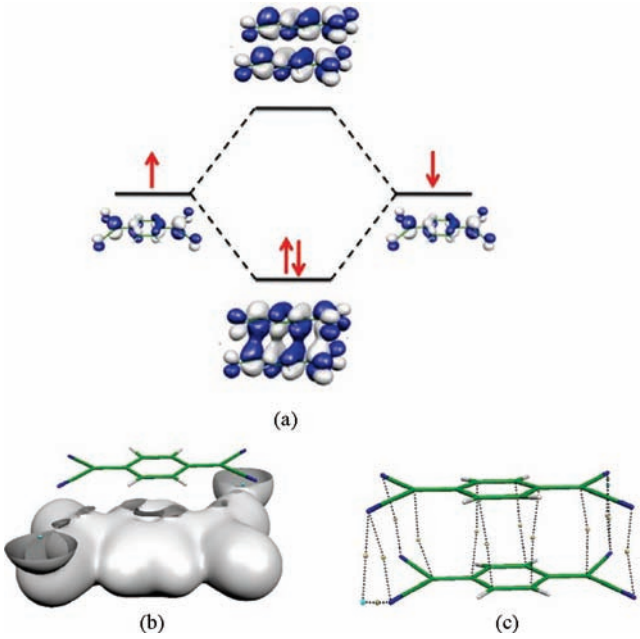

Figure 6. MO diagram of the $K_2[TCNQ]_2$ aggregate (C, green; N, blue; H, white; K, cyan) computed at the crystal geometry by performing the B3LYP/6-31+G(d) calculations and showing how the interaction of the two SOMO orbitals of the $[TCNQ]^{\bullet -}$ anion radicals generate the HOMO and LUMO of the aggregate. (b) Isosurface of 0.05 atomic units of electron density for the aggregate computed at the B3LYP/631+G(d) level, showing the presence of funnels between the two $[TCNQ]^{\bullet -}$ anions for the central atoms, where the bond critical points are located. (There is no cutoff that allows a clear pictorial representation of all funnels.) (c) Position of the 12 (4 N···N, 6 C···C, and 4 N···K) intermolecular bond critical points in the aggregate (white) and the atoms that they link (broken lines).

that the orbital diagram of the CSS is that found in other long-distance bonds and similar to that found in covalent bonds (Figure 6a).

The interaction energy relative to the dissociation into its four fragments is −164.4 and −164.6 kcal/mol for the UB3LYP and RB3LYP calculations, respectively, for the singlet states. The value for the triplet is −157.7 kcal/mol. The $K_2[TCNQ]_2$ aggregate is also found to be stable against its dissociation into two $K^+\cdots[TCNQ]^{\bullet -}$ aggregates in their optimum geometry by −31.4 kcal/mol at the RB3LYP level, −31.6 kcal/mol at the UB3LYP level for the singlet state, and −24.7 kcal/mol for the triplet state. The $K_2[TCNQ]_2$ aggregate was fully optimized at the RB3LYP level and found to be a minimum energy point with a *d* value of 3.748 Å, with the two anions placed in an on-top disposition. The RB3LYP interaction energy for the dissociation into four fragments at the geometry they have in the crystal is −178.4 kcal/mol, that is, 14.0 kcal/mol more stable than the crystal geometry for the aggregate. When the geometry optimization was done at the UB3LYP level, a minimum was also found but had the two anion radicals separated at 5.575 Å, which is too far for their SOMOs to overlap. (The singlet is a OSS state.) The interaction energy of the optimum UB3LYP geometry for the dissociation into four fragments is −188.9 kcal/mol.

For comparison with studies on other long-bonded dimers,[4,9−12] an atoms-in-molecules (AIM) analysis[40,41] located the bond critical points that connect the two $[TCNQ]^{\bullet -}\cdots[TCNQ]^{\bullet -}$ anion radicals in the aggregate (Figure 6b,c). There are 10 intermolecular bond critical points in the aggregate connecting the two anion radicals: 4 N···N, 6 C···C. The intradimer sp C atoms do not contribute because of their very small electron density. The N···N contribution to the intradimer bonding is not reported for $[TCNE]_2^{2-}$ because the nitriles bend away from the nominal planes of the two fragments.[4,7] This is not structurally observed for $[TCNQ]_2^{2-}$.[17,23] Additionally, four N···K bond critical points identify the ionic bonds formed between the anion radicals and the cations in this aggregate. Therefore, the long bond present in between these two anion radicals involved 2 electrons and 20 centers (because each bond critical point in this case involves two centers), that is, is of the 2e/20c type.[42] The N···N and C···C bond critical points have densities of $\sim 4 \times 10^{-3}$ atomic units, being the Laplacian positive. The N···K points also present a positive Laplacian, but the density at the point is 1.2×10^{-2} atomic units.

MCQDPT/CASSCF(2,2) calculations were also done to evaluate the dispersion component in the interaction energy curve for the dissociation of the aggregate into its four

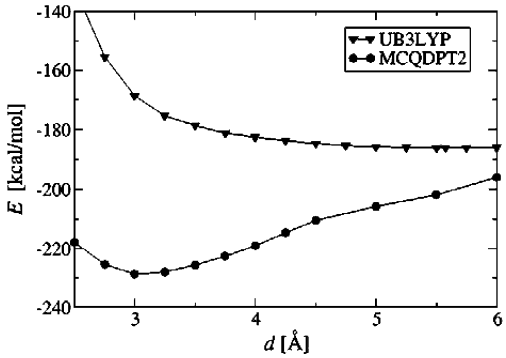

Figure 7. Interaction energy curve, $E(d)$, for the dissociation of one $K_2[TCNQ]_2$ aggregate (in its singlet ground state) into four fragments computed at the UB3LYP and MCQDPT/CASSCF(2,2) levels as a function of intradimer separation (d).

fragments. The 6-31+G(d) basis set was employed in these computations, and the geometry of the aggregate on each point is the optimum computed of the curve at the UB3LYP/6-31+G(d) level because a geometry optimization of an aggregate of this size is currently impossible at the MCQDPT/CASSCF(2,2) level with the available resources. The MCQDPT/CASSCF(2,2)-computed curve as a function of the shortest interfragment $C^+\cdots C$ distance (Figure 7) for the singlet ground state shows only one minimum at ~3.2 Å that is consistent with the experimental results. At this point, the MCQDPT/CASSCF(2,2) interaction energy for the dissociation of the $K_2[TCNQ]_2$ aggregate into four fragments is −222.3 kcal/mol, whereas the interaction energy for the dissociation into two $K^+\cdots[TCNQ]^{\bullet-}$ aggregates is −78.1 kcal/mol; that is, it is a stable aggregate. The two active orbitals in these calculations were chosen to be the HOMO and LUMO that originate from the SOMO of the anion radicals. Their occupations at the minimum of the curve are 1.9 and 0.1, respectively; that is, the singlet is essentially of the CSS type, which is in good agreement with the experimental data and B3LYP results. Along the curve, these occupations continuously vary and become 1.0 and 1.0 above 4.25 Å.

Nature of the $[TCNQ]^{\bullet-}\cdots[TCNQ]^{\bullet-}$ Interactions in Solution. The existence of $[TCNQ]_2^{2-}$ in solution (water) was reported in 1965[14] and more recently also studied in detail in dichloromethane solution.[6] However, an explanation of the stability of these dimers in solution has been elusive. The small enthalpy of formation of these dimers in solution (−10.4 kcal/mol in water[14]) and its solvent dependence indicates that these dimers cannot be associated with $(cation^+)_2[TCNQ]_2^{2-}$ aggregates, whose stability would be much larger and also be solvent-independent. In addition, the presence of dimers in solution at millimolar concentrations, where the anions are solvent-separated and are too distant to form $(cation^+)_2[TCNQ]_2^{2-}$ aggregates, suggests that $cation^+\cdots anion^-$ interactions cannot be the stabilizing interaction that compensates the $[TCNQ]^{\bullet-}\cdots[TCNQ]^{\bullet-}$ repulsion in solution. Therefore, on the basis of recent findings on similar dimers,[43,9,12] the most likely option is the formation of $\{[TCNQ]_2(solvent)_n\}^{2-}$ solvates. The stability of these dimers comes from the $[TCNQ]^{\bullet-}\cdots solvent$ interactions, which should exceed the $[TCNQ]^{\bullet-}\cdots[TCNQ]^{\bullet-}$ repulsion and thus stabilize the formation of $[TCNQ]_2^{2-}$ dimers in solution. The validity of this approach will be computationally evaluated for $\{[TCNQ]_2(H_2O)_n\}^{2-}$ and $\{[TCNQ]_2(CH_2Cl_2)_n\}^{2-}$ aggregates, the two cases in which $[TCNQ]_2^{2-}$ dimers in solution have been reported experimentally. The working principle is similar to that shown in Figure 3, but the two cations are changed by several solvent molecules.[12,43]

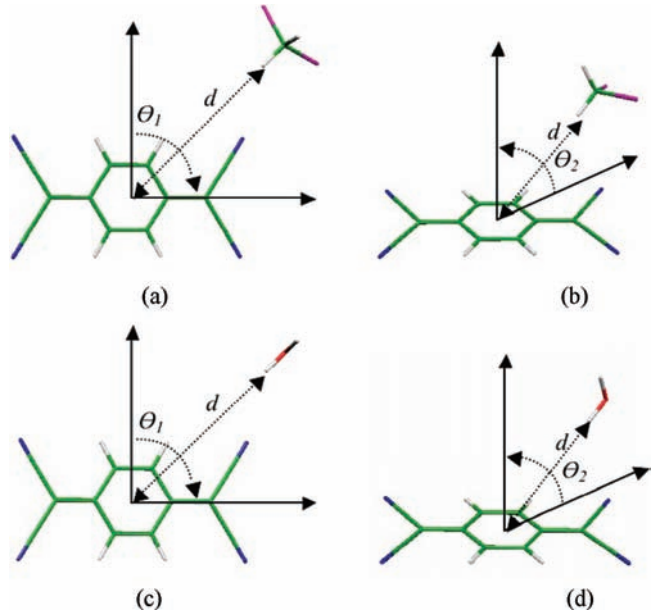

Figure 8. Relative orientations of (a,b) the $[TCNQ]^{\bullet-}$ and CH_2Cl_2 or (c,d) the H_2O molecules. Parts a and c correspond to in-plane orientations (characterized by the value of the Θ_1 angle), whereas parts b and d are for out-of-plane orientations (characterized by the value of the Θ_2 angle). The parameter d is defined as the $H^+\cdots[TCNQ]^{\bullet-}$ center-of-mass (d) distance. In these orientations, the C−H and O−H groups are always collinear with the center-of-mass of the $[TCNQ]^{\bullet-}$ radical.

To make sensible proposals of energetically stable $\{[TCNQ]_2(H_2O)_n\}^{2-}$ and $\{[TCNQ]_2(CH_2Cl_2)_n\}^{2-}$ aggregates, the most stable orientations for the $[TCNQ]^{\bullet-}\cdots H_2O$ and $[TCNQ]^{\bullet-}\cdots CH_2Cl_2$ interaction needs to be identified. We can evaluate the strength and directionality of these two interactions by looking at the interaction energy of a $[TCNQ]^{\bullet-}\cdots H_2O$ and $[TCNQ]^{\bullet-}\cdots CH_2Cl_2$ complex computed at the UB3LYP/6-31+G(d) and UMP2/6-31+G(d) levels for various representative orientations. Given the net negative charge in the $[TCNQ]^{\bullet-}$ fragment, it seems reasonable to expect that the most stable orientations of the solvent molecule should be those where the C−H group of dichloromethane or the O−H group of water points toward the anion radical. This was confirmed by computations. Therefore, only these orientations are focused on.

Two such orientations were evaluated to explore the range of interaction energies for the $[TCNQ]^{\bullet-}\cdots H_2O$ and $[TCNQ]^{\bullet-}\cdots CH_2Cl_2$ interactions: an in-plane orientation where the C−H and O−H groups were placed on the plane of $[TCNQ]^{\bullet-}$ (Figure 8a,c), optimizing the value of the $H^+\cdots TCNQ$ center-of-mass (d) distance for each Θ_1 angle, and an out-of-plane orientation where, for the most stable in-plane orientation, the value of d was optimized for each Θ_2 angle (Figure 8b,d).

The UB3LYP- and UMP2-computed potential energy curves, $E(d)$, for the in-plane and out-of-plane orientations are shown in Figure 9a,b for the $[TCNQ]^{\bullet-}\cdots CH_2Cl_2$ interaction and Figure 9c,d for the $[TCNQ]^{\bullet-}\cdots H_2O$ interaction. The two interactions are energetically stable for all orientations explored in these Figures. The minimum of each in-plane orientation is found at $\Theta_1 = 60°$ in both interactions. Two minima are found in each out-of-plane orientation at 0 and 90°, with the former being more stable. Therefore, both interactions have a similar angular dependence. It is also worth noting the similar strength of the

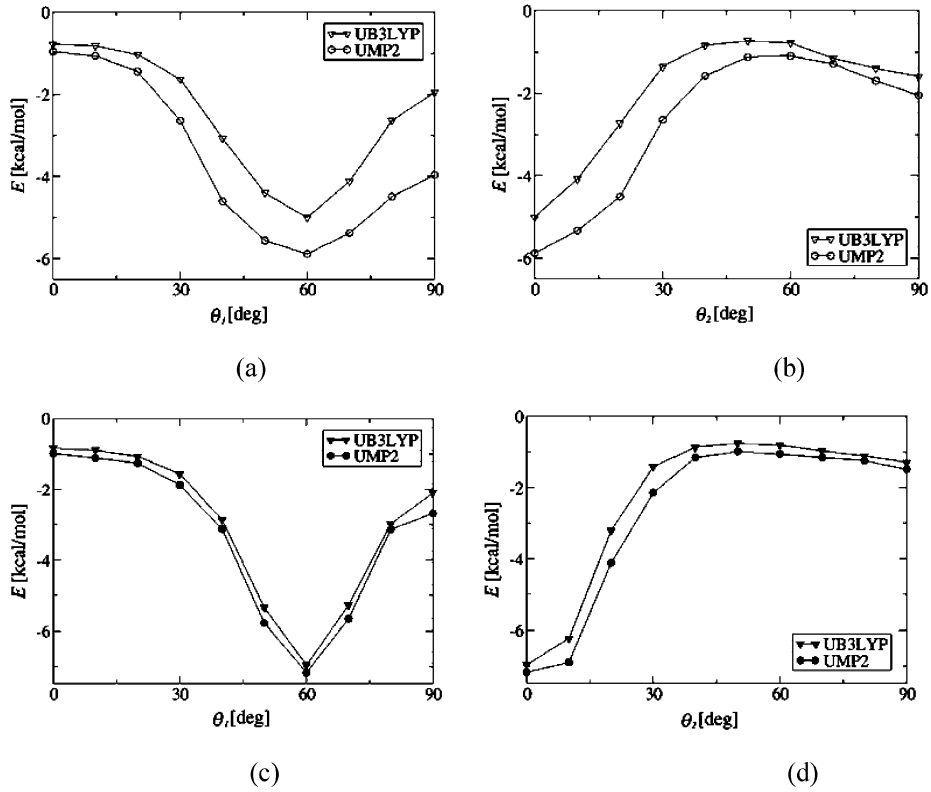

Figure 9. Computed potential energy curves, $E(d)$, for the (a,c) in-plane and (b,d) out-of-plane orientations for the (a,b) $[TCNQ]^{\bullet-}\cdots CH_2Cl_2$ interaction and for the (c,d) $[TCNQ]^{\bullet-}\cdots H_2O$ interaction. See Figure 8 for a view of the geometries for each orientation.

two interactions (~7 kcal/mol), although that for water it is slightly larger (7.2 vs 7.0 kcal/mol). Finally, note the similarity between the UB3LYP and UMP2 evaluations of these strength and angularity, which provides confidence in the results of the UB3LYP geometry optimizations of the $\{[TCNQ]_2(H_2O)_n\}^{2-}$ and $\{[TCNQ](CH_2Cl_2)_n\}^{2-}$ aggregates.

The values of the $[TCNQ]^{\bullet-}\cdots CH_2Cl_2$ and $[TCNQ]^{\bullet-}\cdots H_2O$ interactions obtained before suggest that four dichloromethane or four water molecules placed equatorially in between the two fragments of a π dimer in such a way that each solvent molecule makes two $H\cdots[TCNQ]^{\bullet-}$ interactions are enough to stabilize the aggregate. (These four molecules would make a total of eight interactions of about 7 kcal/mol, totaling about 56 kcal/mol, which is close to the UB3LYP calculated energy for an isolated $[TCNQ]_2^{2-}$ dimer at 3 Å.) Note that the stability of the $[TCNQ]_2^{2-}$ will increase when the dispersion interaction is properly accounted for, as by MCQDPT/CASSCF(2,2) computations, and also if more solvent molecules are added. Given the size of the dimer fragments, the first solvation shell of this dimer will include more than four molecules, but four solvent molecules we will be sufficient for validating the basic considerations.

Consequently, two $\{[TCNQ]_2(H_2O)_4\}^{2-}$ and $\{[TCNQ]_2(CH_2Cl_2)_4\}^{2-}$ aggregates with their solvent molecules placed as described above (Figure 10) were constructed, and their geometry was fully optimized at the RB3LYP/6-31+G(d) level. The optimum geometry is shown in Figure 10a,b; that is, the aggregate presents a clear π-$[TCNQ]_2^{2-}$ disposition, with the shortest distance between the anion radicals of 3.740 Å for $\{[TCNQ]_2(CH_2Cl_2)_4\}^{2-}$ and 3.660 Å for $\{[TCNQ]_2(H_2O)_4\}^{2-}$. However, these minima are metastable by 7.9 kcal/mol at the RB3LYP/6-31+G(d) level (the value of their interaction energy for the dissociation of $\{[TCNQ]_2(CH_2Cl_2)_4\}^{2-}$ into its six fragments), whereas that for $\{[TCNQ]_2(H_2O)_4\}^{2-}$ is 3.0 kcal/mol. The aggregate could be made stable by the addition of more solvent molecules, as was previously done in similar studies on $\{[TTF]_2(CH_2Cl_2)_n\}^{2-}$ and $\{[TCNE]_2(CH_2Cl_2)_n\}^{2-}$ aggregates.[9,12]

The MO diagram of these two solvated aggregates was generated (Figure 10c and Figures S2 and S3 in the Supporting Information) at their optimum geometry. They show the formation of well-separated bonding and antibonding orbitals by combination of the two SOMO orbitals of the anion radicals. Therefore, the $\{[TCNQ]_2(H_2O)_4\}^{2-}$ and $\{[TCNQ]_2(CH_2Cl_2)_4\}^{2-}$ aggregates have a similar geometry and electronic structure as those of the $(cation)_2[TCNQ]_2^{2-}$ aggregates found in the solid state, in accord with their similar properties. Note that when the optimization is done at the UB3LYP/6-31+G(d) level, the π-$[TCNQ]_2^{2-}$ disposition is also preserved, but the shortest distance between the anion radicals in these dimers becomes 5.099 and 4.638 Å, respectively, which is too far to allow any sizable overlap between the anion radical SOMOs.

An AIM analysis was done on the RB3LYP/6-31+G(d) wave function of the $\{[TCNQ]_2(H_2O)_4\}^{2-}$ and $\{[TCNQ]_2(CH_2Cl_2)_4\}^{2-}$ aggregates to locate the position of the bond critical points that connect the two anion radicals in these aggregates (Figure 10d) at their optimum RB3LYP geometry. There are 8 $C\cdots C$ intermolecular bond critical points between the two $[TCNQ]^{\bullet-}$, which describe the long bond properties, and 8 $H\cdots N$ connecting them with the solvent molecules, each associated with an anion−solvent interaction. Therefore, the long bond present between these two anion radicals involves two electrons and 16 centers; that is, it is a 2e/16c bond.[42] The bond critical points for 8 $C\cdots C$ bond components all have densities of $\sim 4 \times 10^{-3}$ atomic units and are Laplacian positive. In contrast with the bonding in the solid state, $N\cdots N$ interactions do not contribute, as the nitriles bend away from the nominal planes of the two fragments, as occurs for $[TCNE]_2^{2-}$.[4,7]

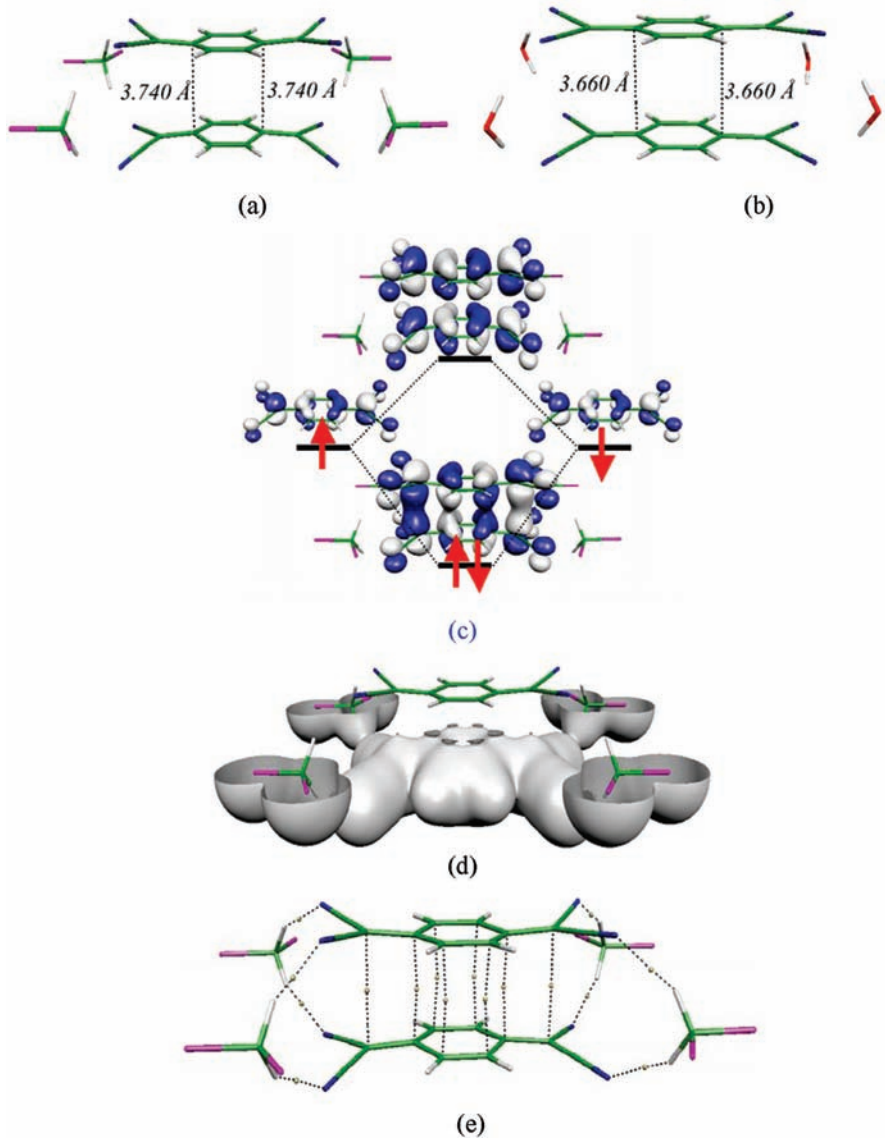

Figure 10. (a) Optimum RB3LYP/6-31+G(d) geometry of the $\{[TCNQ]_2(CH_2Cl_2)_4\}^{2-}$ aggregate. (b) Optimum RB3LYP/6-31+G(d) geometry of the $\{[TCNQ]_2(H_2O)_4\}^{2-}$ aggregate. (c) MO diagram for the $\{[TCNQ]_2(CH_2Cl_2)_4\}^{2-}$ aggregate computed at the RB3LYP/6-31G(d) level, indicating the orbital occupation for the closed-shell singlet state. (d) Isosurface density plot of 0.05 atomic units, showing funnels between the two $[TCNQ]^{\bullet-}$ anions. (e) Position of the 16 (8 C···C and 8 H···N) intermolecular bond critical points in the aggregate (white) and the atoms that they link (broken lines). The shortest distance between the anion radicals is indicated in parts a and b.

The H···N points also present a positive Laplacian, but the density at the point is 1.2×10^{-2} atomic units. These results are very similar to those found in $K_2[TCNQ]_2$ aggregates. Therefore, the $\{[TCNQ]_2(H_2O)_4\}^{2-}$ and $\{[TCNQ]_2(CH_2Cl_2)_4\}^{2-}$ aggregates possess long, multicenter bonds that are similar to those found in $K_2[TCNQ]_2$ aggregates.

Finally, the $E(d)$ curve for the dissociation of $\{[TCNQ]_2(H_2O)_4\}^{2-}$, in its singlet state into its six constituent fragments was computed at the MCQDPT2/CASSCF(2,2) level to test the influence of the dispersion term on the stability of this aggregate. We computed the MCQDPT2/CASSCF(2,2) curve by forcing the separation of the two anion radicals at a given distance (preserving their on-top π disposition) and optimizing at the UB3LYP/6-31+G(d) level the geometry of the aggregate. On the optimum geometry of each point, the MCQDPT2/CASSCF(2,2) interaction energy was computed.[44] To lower the computational cost in these MCQDPT2/CASSCF(2,2) calculations, the 6-31+G(d) was used for the anion radical and the 3-21G basis set was used for the solvent. The MCQDPT2/CASSCF(2,2) potential energy curve obtained for the $\{[TCNQ]_2(H_2O)_4\}^{2-}$ aggregate, Figure 11, is stable at all distances and has a minimum at ~3 Å, with an interaction energy of −39.9 kcal/mol. At the minimum, the $\{[TCNQ]_2(H_2O)_4\}^{2-}$ aggregate is also stable against its dissociation into two $\{[TCNQ](H_2O)_2\}^{-}$ aggregates by −15.9 kcal/mol. The interaction energy for the $\{[TCNQ]_2(CH_2Cl_2)_4\}^{2-}$ aggregate for the dissociation into six fragments was computed at 3.0 Å, and a value of −22.1 kcal/mol was found. Therefore, when dispersion is properly accounted for, four solvent molecules are sufficient to find stable aggregates. The electronic structure of the aggregate is similar to that shown in Figure 10 from the RB3LYP calculations, with an occupation of the HOMO orbital of 1.8 electrons for both the $\{[TCNQ]_2(CH_2Cl_2)_4\}^{2-}$ and the $\{[TCNQ]_2(H_2O)_4\}^{2-}$ aggregates. An AIM analysis of the MCQDPT/CASSCF(2,2) wave function indicated the presence of the same bond critical points discussed for the RB3LYP wave function, with the same characteristics as their

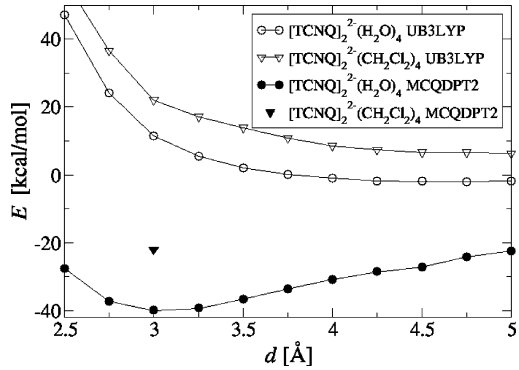

Figure 11. Computed $E(d)$ at the UB3LYP and MCQDPT/CASSCF(2,2) levels as a function of intradimer separation (d) for the dissociation of a $\{[TCNQ]_2(CH_2Cl_2)_4\}^{2-}$ and $\{[TCNQ]_2(H_2O)_4\}^{2-}$ aggregate, in its singlet ground state, into six fragments. To reduce the computational cost, only one point is provided for the MCQDPT interaction energy of the $\{[TCNQ]_2(CH_2Cl_2)_4\}^{2-}$ curve (for $d = 3$ Å) to provide a reference energy because it is expected to have a shape similar to the MCQDPT curve for the $\{[TCNQ]_2(H_2O)_4\}^{2-}$ aggregate.

corresponding ones in the RB3LYP wave function (Figure S2 in the Supporting Information).

Conclusions

The existence of $[TCNQ]_2^{2-}$ dimers in crystals and in solution is computed to originate from $[TCNQ]^{\bullet-}\cdots$cation$^+$ or $[TCNQ]^{\bullet-}\cdots$solvent electrostatic interactions, whose sum exceeds the $[TCNQ]^{\bullet-}\cdots[TCNQ]^{\bullet-}$ repulsions in solution or the sum of the $[TCNQ]^{\bullet-}\cdots[TCNQ]^{\bullet-}$ and cation$^+\cdots$cation$^+$ repulsions in crystals. The energetic balance responsible for their stability has been demonstrated in $K_2[TCNQ]_2$ or $\{[TCNQ]_2(S)_4\}^{2-}$ aggregates ($S = H_2O$, CH_2Cl_2). The long, multicenter two-electron bond present in between two $[TCNQ]^{\bullet-}$ involves 20 centers (4 N$\cdots$N plus 6 C$\cdots$C) in the solid state and 16 C centers in solution because N$\cdots$N interactions do not contribute as the nitriles bend away from the nominal planes of the two fragments, as occurs for $[TCNE]_2^{2-}$.[4,7] As shown by the results of the MCQDPT/CASSCF(2,2) calculations, the electronic ground state of the $[TCNQ]_2^{2-}$ dimers in these clusters is a closed-shell single state with non-negligible contribution of the open-shell singlet. This closed-shell singlet nature of the ground state is similarly reproduced by B3LYP calculations, differently from what was found in $[TCNE]_2^{2-}$ and $[TTF]_2^{2+}$ dimers in the solid and solution.

Acknowledgment. I.G.-Y. and J.J.N. were supported by the Spanish Science and Education Ministry (MAT2008-02032/MAT, BQU2002-04587-C02-02, and UNBA05-33-001, and Ph.D. grant to I.G.-Y.) and the CIRIT (2001SGR-0044 and 2005-PEIR-0051/69). Computer time was also provided by CESCA and BSC. J.S.M. was supported in part by the U.S. NSF (grant no. 0553573) and the DOE (grant no. DE FG 03-93ER45504).

Supporting Information Available: Mulliken atomic spin population for TCNQ, data on all crystal structures presenting $[TCNQ]_2^{2-}$ dimers in the CSD, MO diagrams of the $\{[TCNQ]_2(H_2O)_4\}^{2-}$ aggregate, their electron density, and the position of the intradimer intermolecular bond critical points computed at the RB3LYP/6-31+G(d) level, MO diagrams for $[TCNQ]_2(ClO_4)_2$, their electron density, and the position of the intradimer intermolecular bond critical points computed at the MCQDPT/CASSCF(2,2) level, and the full list of authors for ref 35. This material is available free of charge via the Internet at http://pubs.acs.org.

References and Notes

(1) (a) Miller, J. S.; Epstein, A. J.; Reiff, M. M. *Science* **1988**, *240*, 40. (b) Kahn, O. *Molecular Magnetism*; VCH: New York, 1993.

(2) (a) Miller, J. S.; Epstein, A. J. *Angew. Chem., Int. Ed.* **1994**, *33*, 385. (b) Miller, J. S. *Inorg. Chem.* **2000**, *39*, 4392. (c) Yee, G. T.; Miller, J. S. In *Magnetism: Molecules to Materials*; Miller, J. S., Drillon, M., Eds.; Wiley-VCH: Weinheim, Germany, 2005; Vol. *5*, p 223. (d) Coronado, E.; Galàn-Mascarós, J. R.; Miller, J. S. In *Comprehensive Organometallic Chemistry III*; Crabtree, R. H., Mingos, D. M. P., Eds.; Elsevier: London, 2006; Vol. 12, p 413.

(3) For example, (a) Graja, A. *Low-Dimensional Organic Conductors*; World Scientific: Singapore, 1992. (b) Ferraro, J. R.; Williams, J. M. *Introduction to Synthetic Electrical Conductors*; Academic Press: Orlando, FL, 1987. (c) Hünig, S. *J. Mater. Chem.* **1995**, *5*, 1469. (d) Williams, J. M. *Organic Superconductors (Including Fullerenes): Synthesis, Structure, Properties, and Theory*; Prentice Hall: Englewood Cliffs, NJ, 1992. (e) Ishiguro, T.; Yamaji, K.; Saito, G. *Organic Superconductors*; Springer: New York, 1998.

(4) (a) Novoa, J. J.; Lafuente, P.; Del Sesto, R. E.; Miller, J. S. *Angew. Chem., Int. Ed.* **2001**, *40*, 2540. (b) Del Sesto, R. E.; Miller, J. S.; Novoa, J. J.; Lafuente, P. *Chem.—Eur. J.* **2002**, *8*, 4894. (c) Novoa, J. J.; Lafuente, P.; Del Sesto, R. E.; Miller, J. S. *CrystEngComm* **2002**, *4*, 373.

(5) Jung, Y.; Head-Gordon, M. *Phys. Chem. Chem. Phys.* **2004**, *6*, 2008.

(6) (a) Lu, J.-M.; Rosokha, S. V.; Kochi, J. K. *J. Am. Chem. Soc.* **2003**, *125*, 12161. (b) Jakowski, J.; Simons, J. *J. Am. Chem. Soc.* **2003**, *125*, 16089.

(7) Miller, J. S.; Novoa, J. J. *Acc. Chem. Res.* **2007**, *40*, 189.

(8) Bagnato, J. D.; Shum, W. W.; Strohmeier, M.; Grant, D. M.; Arif, A. M.; Miller, J. S. *Angew. Chem., Int. Ed.* **2006**, *45*, 5326.

(9) Garcia-Yoldi, I.; Novoa, J. J.; Miller, J. S. *J. Phys. Chem. A* **2007**, *111*, 8020.

(10) Garcia-Yoldi, I.; Mota, F.; Novoa, J. J. *J. Comput. Chem.* **2007**, *28*, 326.

(11) Garcia-Yoldi, I.; Miller, J. S.; Novoa, J. J. *Phys. Chem. Chem. Phys.* **2008**, *10*, 4106.

(12) Garcia-Yoldi, I.; Miller, J. S.; Novoa, J. J. *J. Phys. Chem. A* **2009**, *113*, 484.

(13) (a) Goto, K.; Kubo, T.; Yamamoto, K.; Nakasuji, K.; Sato, K.; Shiomi, D.; Takui, T.; Kubota, M.; Kobayashi, T.; Yakusi, K.; Ouyang, J.; Nakasuji, K. *J. Am. Chem. Soc.* **1999**, *121*, 1619. (b) Small, D.; Zaitsev, V.; Jung, Y.; Rosokha, S. V.; Head-Gordon, M.; Kochi, J. K. *J. Am. Chem. Soc.* **2004**, *126*, 13850. (c) Small, D.; Rosokha, S. V.; Kochi, J. K.; Head-Gordon, M. *J. Phys. Chem. A* **2005**, *109*, 11261. (d) Zaitsev, V.; Rosokha, S. V.; Head-Gordon, M.; Kochi, J. K. *J. Org. Chem.* **2006**, *71*, 520. (e) Mota, F.; Miller, J. S.; Novoa, J. J. *J. Am. Chem. Soc.*, published online May 14, 2009, http://dx.doi.org/10.1021/ja9002298.

(14) Boyd, R. H.; Phillips, W. D. *J. Chem. Phys.* **1965**, *43*, 2927.

(15) For example,(a) Reis, A. H., Jr.; Gebert, E.; Miller, J. S. *Inorg. Chem.* **1981**, *20*, 313. (b) Goldberg, S. Z.; Spivack, B.; Stanley, G.; Eisenberg, R.; Braitsch, D. M.; Miller, J. S.; Abkowitz, M. *J. Am. Chem. Soc.* **1977**, *99*, 110. (c) Grossel, M. C.; Evans, F. A.; Hriljac, J. A.; Prout, K.; Weston, S. C. *J. Chem. Soc., Chem. Commun.* **1990**, 1494. (d) Axcondo, M. T.; Ballester, L.; Golhen, S.; Gutierrez, A.; Ouahab, L.; Yartsev, S.; Delhaes, P. *J. Mater. Chem.* **1999**, *9*, 1237. (e) Hynes, R. C.; Morton, J. R.; Preston, K. F.; Williams, A. J.; Evans, F.; Grossel, M. C.; Sutcliffe, L. H.; Weston, S. C. *J. Chem. Soc., Faraday Trans.* **1991**, *87*, 2229. (f) Miller, J. S.; Zhang, J. H.; Reiff, W. M.; Preston, L. D.; Reis, A. H., Jr.; Gerbert, E.; Extine, M.; Troup, J.; Ward, M. D. *J. Phys. Chem.* **1987**, *91*, 4344.

(16) Lü, J.-L.; Rosokha, S. V.; Kochi, J. K. *J. Am. Chem. Soc.* **2003**, *125*, 12161.

(17) Huang, J.; Kingsbury, S.; Kertesz, M. *Phys. Chem. Chem. Phys.* **2008**, *10*, 2625.

(18) Bondi, A. *J. Phys. Chem.* **1964**, *68*, 441.

(19) Allen, F. H. *Acta Crystallogr., Sect. B: Struct. Crystallogr. Cryst. Chem.* **2002**, *58*, 380.

(20) (a) Mikami, S.; Sugiura, K.-I.; Miller, J. S.; Sakata, Y. *Chem. Lett.* **1999**, 413. (b) Zhao, H.; Heinz, R. A.; Dunbar, K. R.; Rogers, R. D. *J. Am. Chem. Soc.* **1996**, *118*, 12844. (c) Harms, R. H.; Keller, H. J.; Nöthe, D.; Werner, M.; Grundel, D.; Sixl, H.; Soos, Z. G.; Metzger, R. M. *Mol. Cryst. Liq. Cryst.* **1981**, *65*, 179. (d) Hoffman, S. K.; Corvan, P. J.; Singh, P.; Sethuklekshmi, C. N.; Metzer, R. M.; Hatfield, W. E. *J. Am. Chem. Chem.* **1983**, *105*, 4608. (e) Dong, V.; Endres, H.; Keller, H. J.; Moroni, W.; Nöthe, D. *Acta Crystallogr.* **1977**, *B33*, 2428.

(21) (a) Zhang, J.; Liable-Sands, L. M.; Rheingold, A. L.; Del Sesto, R. E.; Gordon, D. C.; Burkhart, B. M.; Miller, J. S. *J. Chem. Soc., Chem. Commun.* **1998**, 385. (b) Pokhodnya, K. I.; Bonner, M.; DiPasquale, A. G.; Rheingold, A. L.; Her, J.-H.; Stephens, P. W.; Park, J.-W.; Kennon, B. S.;

Arif, A. M.; Miller, J. S. *Inorg. Chem.* **2007**, *46*, 247. (c) Her, J.-H.; Stephens, P. W.; Pokhodnya, K. I.; Bonner, M.; Miller, J. S. *Angew. Chem., Int. Ed.* **2007**, *46*, 1521. (d) Brook, D. J. R.; Yee, G. T. *Inorg. Chem.* **2006**, *48*, 1406. (e) Wang, G.; Slebodnick, C.; Yee, G. T. *Inorg. Chim. Acta* **2008**, *361*, 3593.

(22) There are examples in the CSD database of $[TCNQ]^{\bullet-}$ forming segregated regular stacks, $[TCNQ]_2^{2-}$ dimers, and $[TCNQ]^{\bullet-}\cdots[TCNQ]^{\bullet-}\cdots[TCNQ]^{\bullet-}$ triads. When dimers or segregated stacks are formed, the adjacent pairs are of the $[TCNQ]^{\bullet-}\cdots[TCNQ]^{\bullet-}$ type, whereas in the last case, they are of the $[TCNQ]^{\bullet-}\cdots[TCNQ]^{0}$ type. See, for instance: Liu, G.-X.; Xu, H.; Ren, X.-M.; Sun, W.-Y. *CrystEngComm* **2008**, *10*, 1574.

(23) Herbstein, F. H.; Kapon, M. *Cryst. Rev.* **2008**, *3*, 74.

(24) (a) Phillips, W. D.; Powell, J. C. *J. Chem. Phys.* **1960**, *33*, 626. (b) Chang, R. *J. Phys. Chem.* **1970**, *74*, 2029. (c) Chesnut, D. B.; Phillips, W. D. *J. Chem. Phys.* **1961**, *35*, 1002.

(25) (a) Itoh, M. *J. Am. Chem. Soc.* **1970**, *92*, 886. (b) Itoh, M. *Bull. Chem. Soc. Jpn.* **1972**, *45*, 1947. (c) Komarynsky, M. A.; Wahl, A. C. *J. Phys. Chem.* **1975**, *79*, 695. (d) Chang, R. *J. Phys. Chem.* **1970**, *74*, 2029.

(26) Lü, J.-M.; Rosokha, S. V.; Kochi, J. *J. Am. Chem. Soc.* **2003**, *125*, 12161.

(27) Gundel, D.; Sixl, H.; Metzger, R. M.; Heiner, N. E.; Harms, R. H.; Keller, H. J.; Nothe, D.; Wehe, D. *J. Chem. Phys.* **1983**, *79*, 3678.

(28) Konno, M.; Ishii, T.; Saito, Y. *Acta Cryst. B:* **1977**, *33*, 763 CSD REFCODE KTCYQM01.

(29) B3LYP is a density functional obtained by taking the three-parameter nonlocal exchange functional of Becke and the nonlocal correlation functional of Lee−Yang−Parr:(a) Becke, A. D. *J. Chem. Phys.* **1993**, *98*, 5648. (b) Lee, C.; Yang, W.; Parr, R. G. *Phys. Rev. B* **1988**, *37*, 785.

(30) The CASSCF(2,2) method performs a multiconfiguration self-consistent field calculation using a (2,2) complete active space (that is, using all determinants generated from a two-electrons and two-orbitals active space). The methodology is described in: Szabo, A.; Otslund, N. S. *Modern Quantum Chemistry*; Macmillan: New York, 1982; p 258.

(31) Nakano, H.; Nakayama, K.; Hirao, K.; Dupuis, M. *J. Chem. Phys.* **1997**, *106*, 4912.

(32) The MCQDPT/CASSCF(2,2) method performs multiconfigurational perturbation calculation on a multiconfigurational CASSCF(2,2) wavefunction using the MCQDPT method.

(33) Roos, B. O.; Andersson, K.; Fulscher, M. K.; Malmqvist, P.-A.; Serrano-Andres, L.; Pierloot, K.; Merchan, M. *Adv. Chem. Phys.* **1996**, *93*, 219.

(34) A basis set built by adding diffuse functions to the 6-31G(d) basis set. The latter is described in: Ditchfield, R.; Hehre, W. J.; Pople, J. A. *J. Chem. Phys.* **1971**, *54*, 724.

(35) Frisch, M. J., et al; *Gaussian 03*, revision C.02; Gaussian, Inc.: Wallingford, CT, 2004.

(36) Schmidt, M. W.; Baldridge, K. K.; Boatz, J. A.; Elbert, S. T.; Gordon, M. S.; Jensen, J. H.; Koseki, S.; Matsunaga, N.; Nguyen, K. A.; Su, S. J.; Windus, T. L.; Dupuis, M.; Montgomery, J. A. *J. Comput. Chem.* **1993**, *14*, 1347.

(37) Boys, S. F.; Bernardi, F. *Mol. Phys.* **1970**, *19*, 553.

(38) For example, Johansen, H. *Int. J. Quantum Chem.* **1975**, *9*, 459.

(39) Grossel, M. C.; Weston, S. C. *Chem. Commun.* **1992**, 1510 CSD REFCODE KIZBOC.

(40) Bader, R. F. W. *Atoms in Molecules: A Quantum Theory*; Clarendon Press: Oxford, U.K., 1990.

(41) The calculations were done with the program PROAIM. See: Biegler-Konig, F. W.; Bader, R. F. W.; Tang, T. H. *J. Comput. Chem.* **1982**, *3*, 317.

(42) As recently shown, the character of the long bond is properly established by looking at the number of unpaired electrons on each ion radical fragment and the atoms connected by bond critical points.[13e]

(43) Carvajal, M. A.; Garcia-Yoldi, I.; Novoa, J. J. *THEOCHEM* **2005**, *727*, 181.

(44) As the difference between the energy of aggregate at this point and when the fragments are separated at 200 Å, thus minimizing the size-consistent error of the MCQDPT/CASSCF(2,2) calculation.

JP901930S